# Mutations that promote furin-independent growth of Semliki Forest virus affect p62–E1 interactions and membrane fusion

Xinyong Zhang, Margaret Kielian*

Department of Cell Biology, Albert Einstein College of Medicine, Bronx, N.Y. 10461 United States

## Abstract

The enveloped alphavirus Semliki Forest virus (SFV) infects cells via a low pH-triggered membrane fusion reaction mediated by the E1 protein. E1's fusion activity is regulated by its heterodimeric interaction with a companion membrane protein E2. Mature E2 protein is generated by furin processing of the precursor p62. Processing destabilizes the heterodimer, allowing dissociation at acidic pH, E1 conformational changes, and membrane fusion. We used a furin-deficient cell line, FD11, to select for SFV mutants that show increased growth in the absence of p62 processing. We isolated and characterized 7 such *pci* mutants (p62 cleavage independent), which retained the parental furin cleavage site but showed significant increases in their ability to carry out membrane fusion in the p62 form. Sequence analysis of the *pci* mutants identified mutations primarily on the E2 protein, and suggested sites important in the interaction of p62 with E1 and the regulation of fusion.
© 2004 Elsevier Inc. All rights reserved.

*Keywords:* Membrane fusion; Alphavirus; Protein processing; Semliki Forest virus; Furin; Endocytosis; Virus entry

## Introduction

Virus membrane fusion proteins are critical for the infection pathway of enveloped animal viruses (Blumenthal et al., 2003; Eckert and Kim, 2001; Hernandez et al., 1996). Such fusion proteins must be regulated to ensure that the membrane fusion reaction occurs at the correct time and place to successfully mediate virus infection. The enveloped alphavirus Semliki Forest Virus (SFV) infects target cells by endocytic uptake in clathrin-coated vesicles (DeTulleo and Kirchhausen, 1998; Helenius et al., 1980; Marsh and Helenius, 1980; Sieczkarski and Whittaker, 2002). The low pH of the endocytic compartment then triggers fusion of the virus membrane with the endosome membrane (reviewed in Kielian, 1995; Kielian et al., 2000). The SFV membrane contains approximately 2–50 kDa transmem-brane proteins that mediate these entry and fusion steps (reviewed in Schlesinger and Schlesinger, 2001; Strauss and Strauss, 1994). E2 is the receptor-binding protein and appears to interact with several receptor candidates to allow endocytic uptake by a wide range of host cells (Strauss and Strauss, 1994). The E1 protein mediates the membrane fusion reaction and contains the virus fusion peptide, a highly conserved hydrophobic domain that inserts into the target membrane (Gibbons et al., 2004a; Kielian et al., 1996). Although at neutral pH the virus particle contains heterodimers of E2 and E1, during membrane fusion E1 rearranges to a highly stable E1 homotrimer structure that is critical for the membrane fusion reaction (Gibbons et al., 2004b; Kielian et al., 1996; Wahlberg et al., 1992).

Recent structural studies have greatly advanced our knowledge of the E1 protein, the alphavirus particle, and the disposition of the envelope proteins in the virion. Cryo-electron microscopy and computer reconstruction studies showed that the envelope glycoproteins are organized with $T = 4$ icosahedral symmetry on the virus particle (Cheng et al., 1995; Fuller et al., 1995). The glycoprotein layer of the

---

* Corresponding author. Department of Cell Biology, Albert Einstein College of Medicine, 1300 Morris Park Avenue, Bronx, NY, 10461. Fax: +1 718 430 8574.
*E-mail address:* kielian@aecom.yu.edu (M. Kielian).

virus particle is composed of a spiky projecting domain and a skirt domain covering the viral lipid bilayer (Mancini et al., 2000). Native E1 is an elongated 3-domain molecule with the fusion peptide in domain II at one tip of the molecule, and the transmembrane domain at the other end (Lescar et al., 2001). Fitting of the E1 structure into the cryo-EM density showed that E1 has a tangential orientation and interacts in an icosahedral scaffold to form most of the skirt domain, while E2 forms the projecting spike structures at the 3-fold and quasi-3-fold axes (Lescar et al., 2001; Pletnev et al., 2001). E2 covers most of the E1 molecule on the assembled particle, and fitting studies reveal two major heterodimer interaction sites on the E1 protein (Lescar et al., 2001; Zhang et al., 2002). E2 directly contacts E1 at the tip of domain II including the fusion peptide, and in the region of domain III leading to the E1 transmembrane domain. As the structure of E2 has not yet been solved, the regions of E2 that contact E1 are not well understood. It is clear, however, that fusion involves major rearrangements in the E2–E1 dimer. E1 reorients vertically, inserts its fusion peptide into the target membrane, trimerizes, and refolds to form a hairpin-type structure with the fusion peptide and the transmembrane domain at the same end of the molecule (Gibbons et al., 2003, 2004b). Thus, consideration of the virus architecture and E1 homotrimer structure would suggest that the heterodimeric interaction of E1 with E2 would act to prevent fusion and could be important for its regulation.

Extensive biochemical and mutagenesis studies have directly demonstrated that E2 does play an important regulatory role during fusion. Treatment of SFV at low pH dissociates the E2–E1 dimer (Wahlberg and Garoff, 1992), and kinetic studies have demonstrated that dimer dissociation is an early event that precedes formation of the E1 homotrimer and membrane fusion (Justman et al., 1993; Wahlberg and Garoff, 1992; Wahlberg et al., 1992). An SFV mutant termed *fus-1* has a pH threshold for fusion of approximately pH 5.3, compared to the normal wild type (wt) SFV threshold of approximately pH 6.2 (Glomb-Reinmund and Kielian, 1998; Kielian et al., 1984). This phenotype is caused by the mutation of E2 threonine 12 to isoleucine, which stabilizes the E2–E1 dimer, inhibits its dissociation at low pH, and thus blocks the formation of the E1 homotrimer at the normal pH of fusion (Glomb-Reinmund and Kielian, 1998; Kielian et al., 1984). E2 is initially synthesized as a precursor termed p62 that is endoproteolytically processed late in the biosynthetic pathway to produce mature E2 and the peripheral polypeptide E3. The heterodimer forms early during the biogenesis of p62 and E1 within the ER and is required for the correct folding and transport of E1 (Andersson et al., 1997; Carleton et al., 1997; Molinari and Helenius, 2000). Interestingly, the p62–E1 dimer is more acid-stable than the mature E2–E1 dimer (Wahlberg et al., 1989), and it has been suggested that the stable p62 dimer interaction protects E1 from the mildly acidic pH of the trans-Golgi network (Andersson et al., 1997). p62-containing

viruses can be triggered to fuse but require treatment at considerably more acidic pH (approximately 5.0), which triggers the dissociation of the heterodimer and the formation of the E1 homotrimer (Salminen et al., 1992; Smit et al., 2001; Zhang et al., 2003). p62-containing viruses are less infectious due to their decreased fusion activity at the normal physiological pH range of the early endosome compartment (Salminen et al., 1992; Smit et al., 2001; Zhang et al., 2003). Thus, while E2 is not directly involved in virus fusion, in both its precursor and mature forms it acts as a critical companion protein to regulate the fusion activity of E1.

Several different systems have been used to study the role of p62 processing in alphavirus fusion and infection. Processing has been blocked by direct mutation of the p62 furin cleavage site (Davis et al., 1995; Jain et al., 1991; Lobigs and Garoff, 1990; Salminen et al., 1992), or by an E2 mutation that leads to carbohydrate addition near the cleavage site (Russell et al., 1989). While these mutations have been very important in demonstrating the role of p62 in regulating E1, their phenotypes are complicated by deleterious effects of the mutations on virus-receptor binding (Klimstra et al., 1999; Salminen et al., 1992). An alternative method involves the propagation of virus in a cell line that is deficient in furin, the cellular enzyme required for p62 processing. We have used the furin-deficient CHO cell line FD11 to produce p62 virus containing the wt sequence (Zhang et al., 2003). The wt/p62 virus showed efficient binding to the cell surface receptor. This system demonstrated the role of furin in p62 processing and the acid-shifted phenotype of wt/p62 virus dimer dissociation, E1 trimerization, and fusion. As predicted from the fusion phenotype, the infectivity of the p62 virus and the growth of SFV on FD11 cells were inhibited. The FD11 cells thus provide a system to select for mutations that can overcome the growth defect caused by lack of p62 processing of wt virus.

Here, we present the results of such a selection for p62 cleavage-independent SFV mutants, which we have termed *pci* mutants. Seven independent *pci* mutants were isolated and characterized. All seven mutants retained normal p62 processing in furin-containing cells and remained unprocessed in FD11 cells. Fusion assays indicated that the increased replication of mutant viruses in FD11 cells was due to their ability to fuse at a higher pH in the unprocessed form. This increased fusion activity correlated with a less stable heterodimer interaction and a higher pH threshold for E1 homotrimer formation. These mutations thus suggest sites involved in the regulatory interactions of p62 and E1.

## Results

### Isolation of p62-cleavage-independent SFV mutants

We have previously demonstrated that furin is the authentic cellular endoprotease for SFV p62 processing,

and that this processing is blocked in furin-deficient FD11 cells (Zhang et al., 2003). wt SFV shows decreased growth on FD11 cells compared to wt CHO cells, and was unable to form plaques on FD11 cells (data not shown). We therefore made use of this system as a novel method to select for SFV mutants that grow more efficiently on FD11 cells and bypass the negative effects of the absence of p62 processing. For the selection, 10 parallel plates of FD11 cells were infected with wt SFV at the low MOI of 0.01 PFU per cell, and the progeny virus was collected after 15 h at 37 °C. This incubation time permits multiple rounds of secondary infection and showed maximal difference in virus production between cells with and without furin (Zhang et al., 2003). The p62-containing progeny virus stocks were used to perform a new cycle of infection, and the selection process was carried out for a total of 10 rounds. The resulting 10 independent selected virus stocks all showed plaque formation on FD11 cells. Interestingly, the stock from selection 4 had the highest virus titer and the largest plaques on FD11 cells. Mutants were plaque-purified twice on FD11 cells, expanded in FD11 cells, and the final titer determined on BHK cells. Selections 3, 9, and 10 did not produce viable isolates in several attempts. The 7 isolated mutant viruses were termed p62-cleavage-independent (*pci*) mutants 1, 2, 4, 5, 6, 7, and 8.

### Envelope protein processing in CHO and FD11 cells

The observation that the *pci* mutants formed plaques on FD11 cells suggested that the mutants had more efficient growth properties than wt SFV. This could be due to increased fusion of the p62 form, or to processing of the *pci* p62 subunit by an alternative mechanism. To test for the latter possibility, the expression and processing of virus envelope proteins were characterized by pulse-chase experiments in CHO and FD11 cells infected with wt or *pci* mutants. Virus released in the chase media was immunoprecipitated with a polyclonal antibody against the SFV envelope proteins, and the samples were analyzed by SDS-PAGE (Fig. 1). As described above, wt SFV p62 was processed efficiently in CHO cells (C lane) and the processing was inhibited in FD11 cells (F lane). All seven *pci* mutants showed efficient p62 processing in CHO cells (C) and no detectable p62 processing in FD11 cells (F). Thus, the increased growth of the 7 *pci* mutants on FD11 cells was not due to the use of an alternative processing mechanism, suggesting that the *pci* mutants may have altered fusion properties.

Interestingly, E1s, a previously described truncated form of the E1 protein (Duffus et al., 1995; Lu et al., 2001; Zhao and Garoff, 1992), was often observed in the media from CHO cells infected with *pci* mutants, as shown by the increased ratio of E1/E2 in these samples (Fig. 1). Little E1s was produced from CHO cells infected with wt virus, or from FD11 cells infected with wt or *pci* mutants. The generation of wt E1s is strongly pH dependent, with optimal cleavage occurring at an extracellular pH lower than 7.0 for
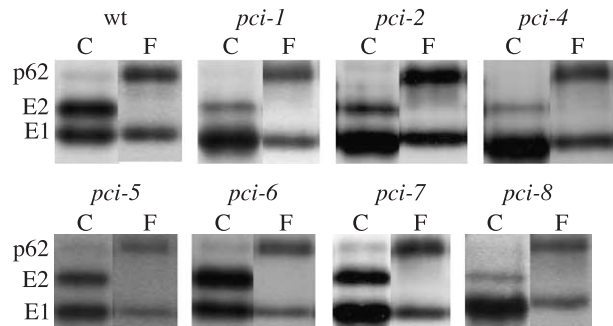


Fig. 1. Membrane protein processing of wt SFV and mutant viruses in CHO and FD11 cells. wt CHO (C) and furin-deficient FD11 cells (F) were infected with wt SFV or the indicated *pci* mutant virus at a multiplicity of 10 PFU per cell for 2 h at 37 °C. Cells were further incubated for 6 h, pulse-labeled with [$^{35}$S]methionine-cysteine for 20 min and chased for 5 h in the absence of label, all at 37 °C. The chase media were collected and immunoprecipitated with a polyclonal antibody against the SFV envelope proteins. The samples were analyzed by SDS-PAGE and fluorography. The data are a representative example of three experiments.

BHK cells (Lu et al., 2001). However, the release of E1s from mutant-infected CHO cells did not appear to be due to the pH of the chase media, which was maintained at pH 7.5 for all samples, and might instead reflect an alteration in the E1–E2 interaction in the *pci* mutants. Variations in the amount of labeled virus proteins recovered from FD11 cells were observed for several mutants, but were not characterized further.

### Sequence analysis of the pci mutants

To identify the amino acid alterations in the *pci* mutants, RNA was isolated from virus produced in FD11 cells, reverse-transcribed, and the cDNA amplified by PCR. The region encoding the envelope proteins was sequenced and all mutations confirmed by an independent RT-PCR reaction. We identified a total of 12 transitions (2 UC, 4 CU, 5 AG, 1 GA) and 2 transversions (1 CA, 1 UA). No mutagen was used and thus these substitutions reflect RNA polymerase errors. Each *pci* mutation was the result of a single nucleotide change (Fig. 2). There were no mutations in E3, and two mutations in E1. All of the remaining mutations were located in the N-terminal half of the E2 protein. *pci-1* has two mutations (E2 Ala121Glu and Arg244Gly); *pci-2* and *pci-6* have the same single point mutation (E2 His170Tyr); *pci-4* has three mutations (E2 Asn77Asp, Leu221Gln, and Arg244Lys); *pci-5* has two mutations (E2 His170Tyr and E1 Thr159Ala); *pci-7* has three mutations (E2 Arg250Gly and E1 Val11Ala and Thr159Ala); and *pci-8* has two mutations (E2 Asn7Asp and His170Tyr). Since *pci-2* and *pci-6* were identical, further characterization of this pair was only performed for *pci-6*. The sequence data confirmed that the original furin cleavage site was retained for all 7 *pci* mutants, in keeping with the unaltered p62 processing observed in CHO cells.
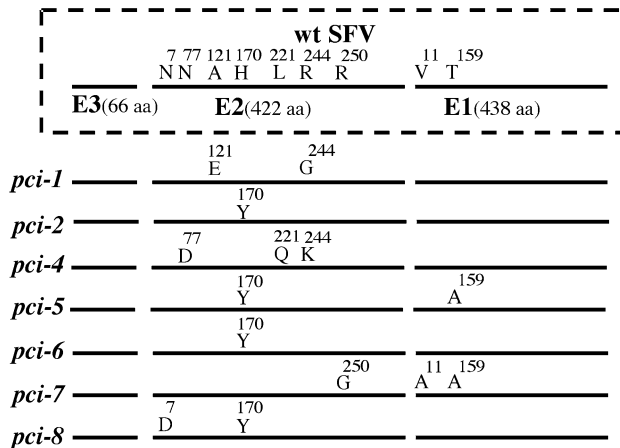
Fig. 2. Comparison of the amino acid sequence of the envelope proteins of wt SFV and *pci* mutants. The position and amino acid residue of all mutations are listed with the corresponding wt SFV sequence. The schematic diagram used to illustrate the envelope proteins is not proportional to their actual size.

## Virus growth kinetics

To characterize the phenotype of the *pci* mutants, we first compared their growth kinetics with those of wt SFV in FD11 and CHO cells. To permit more efficient and equivalent primary infection, cells were infected using stocks of wt/E2 or *pci*/E2 produced in BHK cells. Low multiplicity infection (MOI = 0.01 PFU/cell) was used so that the ability of the progeny virus to reinfect cells could be assessed. At the indicated times post-infection, the media were collected and the progeny virus titer in the media was determined by plaque assay on BHK cells. While the progeny virus from FD11 cells will be in the p62 form, it will infect and plaque relatively efficiently on BHK cells due to cleavage by endogenous furin during virus uptake (Zhang et al., 2003). Comparison of wt and *pci* mutant growth on FD11 cells showed that the *pci* mutants had a growth advantage over the wt virus (Fig. 3A), as predicted by the mutants' ability to form plaques on FD11 cells. Even during the first 10 h of infection in FD11 cells, the mutants produced titers 1–2 logs higher than the wt virus, with *pci-4* showing the most efficient growth. Since at these early infection times most of the progeny virus is derived from the primary infection, this result suggests that the initial infection of FD11 cells by the E2 form of the *pci* mutants may be more efficient than wt virus, and/or that the progeny *pci*/p62 virus is more efficient in plaquing on BHK cells than the wt. By 24 h post-infection, the titer of wt SFV was about $10^5$ PFU/ml, whereas the titer of *pci-4* was about $10^8$ PFU/ml and the titers of the other five *pci* mutants were about $10^7$ PFU/ml. Notably, the titer of *pci-4* on FD11 cells at 30 h post-infection was about the same as that of wt SFV on CHO cells (Fig. 3B and Zhang et al., 2003). Thus, the mutants displayed a strongly increased growth phenotype during secondary infection in the absence of furin cleavage.
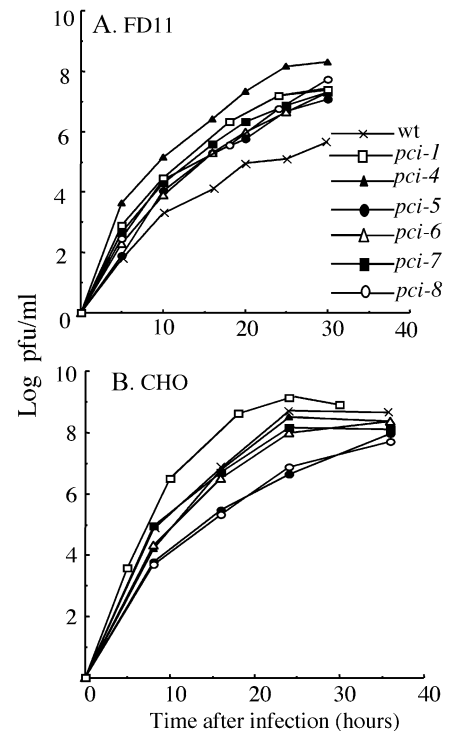


Fig. 3. Growth kinetics of wt SFV and *pci* mutants on CHO and FD11 cells. FD11 (A) and CHO (B) cells were infected with wt/E2 and *pci*/E2 at a multiplicity of 0.01 PFU/cell for 90 min at 37 °C. The cells were then washed twice and the incubation was continued for the indicated times after infection. The titer of virus released in the medium was determined by plaque assay on BHK cells.

We also compared the growth properties of mutants and wt SFV on control CHO cells (Fig. 3B). In furin-containing cells, *pci-1*, *-4*, *-6*, and *-7* grew as efficiently as wt SFV, whereas *pci-5* and *-8* grew more slowly although they reached wt levels by ~36 h. Interestingly, *pci-6*, *pci-5*, and *pci-8* all have the E2 H170Y mutation, suggesting that the other mutations on *pci-5* (T159A) and *pci-8* (N7D) are responsible for their decreased growth efficiency. A comparison of the final titers of wt and *pci* viruses in FD11 and CHO cells showed that the ratio of FD11 titer to CHO titer was 6- to 360-fold higher for the *pci* mutants than the ratio for wt SFV (Table 1). Taken together, these data indicated that the *pci* mutations allowed more efficient

Table 1
Peak titers of wt SFV and *pci* mutants grown on CHO and FD11 cells[a]

| Virus | Titer (log PFU/ml) | | PFU ratio |
|---|---|---|---|
| | CHO | FD11 | (FD11/CHO) |
| Wt | 8.69 | 6.20 | 0.003 |
| *pci-1* | 9.15 | 7.38 | 0.017 |
| *pci-4* | 8.5 | 8.2 | 0.500 |
| *pci-5* | 7.96 | 7.30 | 0.217 |
| *pci-6* | 8.36 | 7.69 | 0.217 |
| *pci-7* | 8.18 | 7.3 | 0.154 |
| *pci-8* | 7.72 | 7.75 | 1.076 |

[a] FD11 and CHO cells were infected with wt/E2 and *pci*/E2 SFV as in Fig. 3, and the maximal final titer was determined by plaque assay on BHK cells.

infection when the virus was in the unprocessed p62 form. The *pci* mutations did not show strong effects when the virus was in the processed E2 form.

## Membrane fusion activity of the pci mutants

To investigate if the growth advantage of the *pci* mutants on FD11 cells was due to an increased fusion ability of the unprocessed virus, we used the virus–cell membrane fusion assay described previously (Vashishtha et al., 1998). p62 virus stocks (Fig. 4) or E2 virus stocks (Fig. 5) were produced in FD11 or BHK cells, respectively. These viruses were pre-bound to BHK cells on ice and the fusion reaction was triggered by treatment with medium at the indicated pH for 3 min at 37 °C. Fusion was scored by immunofluorescence identification of infected cells, and normalized to the maximal fusion obtained for each virus stock. As reported previously (Zhang et al., 2003), wt/p62 fusion was strongly inhibited at the usual pH threshold of 6.2, and required treatment below pH 5.0 to trigger detectable fusion, with maximal fusion observed at pH 4.5 (Fig. 4, black bars). In contrast, the p62 form of all of the mutants showed significant fusion above pH 5.0 (Fig. 4, white bars). *pci-1* showed more than 20% of its maximum fusion level at pH 5.4 (Fig. 4A). *pci-5*, *-6*, and *-7* all have more than 30% of maximum fusion at pH 5.4 (Figs. 4C, D, and E). *pci-8* has more than 60% of maximum fusion at pH 5.2 (Fig. 4F).
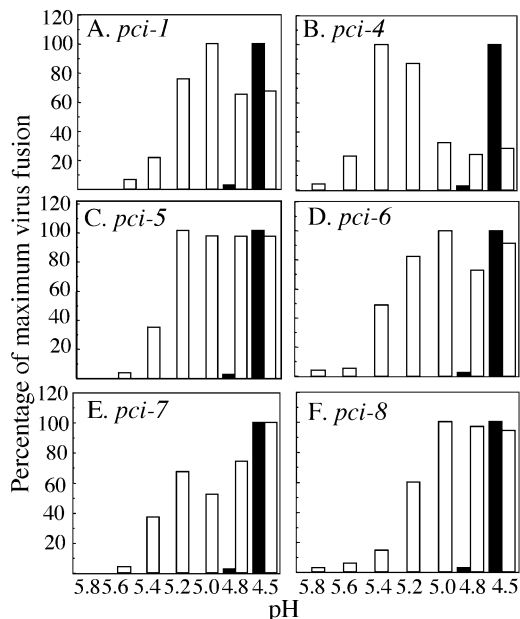


Fig. 4. pH dependence of fusion of p62-containing wt SFV and *pci* mutants. Unprocessed wt/p62 (black bars) and *pci*/p62 viruses (white bars) were produced by growth in FD11 cells. Serial dilutions of virus were absorbed to BHK cells on ice, and virus–plasma membrane fusion was triggered by treatment with medium of the indicated pH for 3 min at 37 °C. Cells were further incubated at 28 °C for 18 h in the presence of 20 mM NH₄Cl to prevent secondary infection. Virus-infected cells were then scored by immunofluorescence and the results expressed as the percentage of maximum fusion for each virus.
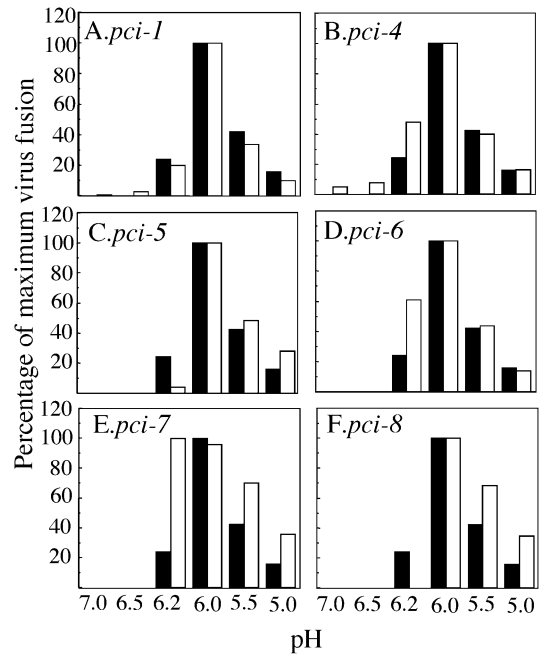


Fig. 5. pH dependence of fusion of E2-containing wt SFV and *pci* mutants. Processed, E2-containing wt SFV (black bars) and *pci* viruses (white bars) were produced by growth in BHK cells. The pH dependence of virus–plasma membrane fusion was determined as described in the legend to Fig. 4.

Interestingly, *pci-4* showed its maximal fusion activity at pH 5.4, a higher fusion threshold than any other *pci* mutant and in keeping with *pci-4* showing the most efficient growth in FD11 cells (Fig. 3A). The fusion activity of *pci-4* declined below approximately pH 5.2, presumably reflecting the sensitivity of this mutant to acid inactivation.

The fusion activities of processed E2 viruses were similarly evaluated (Fig. 5). The results showed that all the *pci*/E2 viruses (Fig. 5, white bars) have maximum fusion ability at pH 6.0 and show acid inactivation/decreased fusion at lower pH, similar to the wt/E2 virus (Fig. 5, black bars). In addition, *pci-4*, *-6*, and *-7* displayed quite efficient fusion activity at higher pH (Figs. 5B, D, and E). In contrast, *pci-5* and-*8*, which both grow less efficiently on CHO cells, show decreased fusion activity at pH 6.2 compared to wt virus (Figs. 5C and F).

Thus, the efficient growth of *pci* mutants on FD11 cells in the absence of p62-processing correlates with their ability to overcome the membrane fusion defect of unprocessed wt virus at the normal physiological pH range of the endosome compartment.

## Biochemical assays of envelope protein conformational changes of the pci mutants

A key step in SFV fusion involves the formation of a stable E1 homotrimer at low pH (Kielian et al., 1996; Wahlberg and Garoff, 1992). Our previous studies demonstrated that wt/p62 requires treatment at a more acidic pH to trigger E1 trimerization, similar to the pH shift of the virus

fusion reaction (Zhang et al., 2003). Since we observed the strongest growth and fusion phenotypes with *pci-4*, we selected this mutant for further analysis of the low pH-dependent conformational changes in the virus envelope proteins. To assay E1 homotrimer formation, radiolabeled *pci-4* virus and wt SFV were produced in FD11 cells or BHK cells. These viruses were treated at the indicated pH in the presence of liposomes at 37 °C for 5 min. Formation of the SDS-resistant E1 homotrimer was analyzed by SDS-PAGE and quantitated by phosphorimager analysis. The processed E2 forms of wt and *pci-4* showed similar efficiency and pH dependence of E1 homotrimer formation, with about 40% of the total E1 forming trimers during treatment at pH 6.2 (Fig. 6A). As previously observed (Zhang et al., 2003), wt/p62 virus required very low pH to trigger trimer formation and maximal trimerization was only about 25% efficient at pH 5.0 (Fig. 6B). In contrast, homotrimer formation of *pci-4*/p62 was triggered more efficiently at a higher pH, showing about 40% conversion at pH 5.8 and 60% at pH 5.5 (Fig. 6B).

SFV E1 homotrimer formation and membrane fusion are controlled by the pH-sensitive interaction of the p62/E2 protein with E1, and the dimer is more acid-labile in the processed E2 form (Wahlberg et al., 1989). The increased fusion and E1 homotrimer formation of unprocessed *pci-4* suggested that its E2 mutations acted by destabilizing the
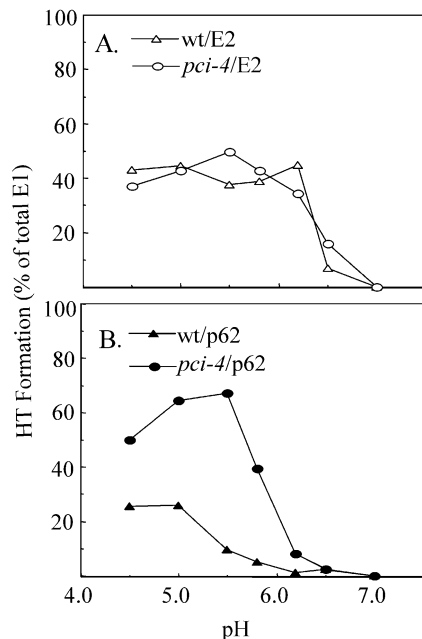


Fig. 6. pH dependence of E1 homotrimer formation for processed and unprocessed wt SFV and *pci-4* mutant. [$^{35}$S]methionine-cysteine-labeled wt and *pci-4* viruses were prepared in the E2 form in BHK cells (A. E2) or in the p62 form in FD11 cells (B. p62). Gradient-purified viruses were mixed with 0.8 mM complete liposomes and treated for 5 min at 37 °C at the indicated pH. Samples were solubilized in SDS-sample buffer for 3 min at 30 °C to preserve the E1 homotrimer, and analyzed by SDS-PAGE and phosphorimaging. Homotrimer formation was expressed as a percentage of the total E1 in each sample.
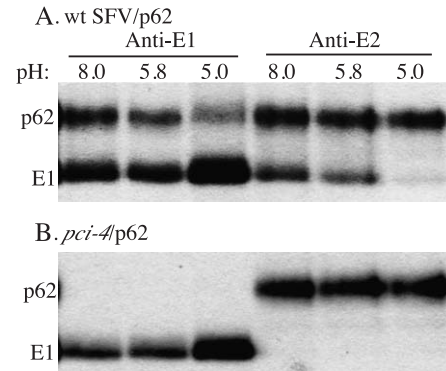


Fig. 7. Dimer stability of wt/p62 and *pci-4*/p62 viruses. To characterize the stability of p62/E1 heterodimer, radiolabeled viruses were prepared in FD11 cells as for Fig. 6B. Viruses were treated at the indicated pH for 10 min on ice, solubilized in 1% Triton X-100, immunoprecipitated with anti-E1 mAb E1-1 or anti-E2 mAb E2-3, and analyzed by SDS-PAGE.

p62–E1 dimer. We compared the dimer association properties of wt/p62 and *pci-4*/p62 viruses by co-immunoprecipitation analysis of the p62 and E1 proteins. Radiolabeled viruses were treated at the indicated pH, solubilized, immunoprecipitated at neutral pH with anti-E1 or anti-E2 monoclonal antibodies, and analyzed by SDS-PAGE. As predicted (Wahlberg et al., 1989), the wt/p62 heterodimer was very stable and dissociation was only observed at pH 5.0 (Fig. 7A). In contrast, the *pci-4* dimer was easily dissociated by detergent solubilization, and no dimer was recovered even at pH 8.0 (Fig. 7B). Using the same assay, the processed wt E2–E1 dimer was stable at neutral pH and dissociated at acidic pH, while the *pci-4* E2–E1 dimer was dissociated by detergent treatment at all pH values tested (data not shown).

## Discussion

Infection by Semliki Forest virus is strongly inhibited by the replacement of E2 with p62 in virus produced from FD11 cells (Zhang et al., 2003). This block to infection is due to the dramatic shift in the pH dependence of membrane fusion for p62-containing virus, while in contrast the receptor binding activity of the p62 virus is as efficient as wt (Zhang et al., 2003). The FD11 cells provided a novel selection for virus mutants containing what have been termed "resuscitating" mutations (Smit et al., 2001), suppressor mutations that enhance the growth and fusion of the p62 form of the virus. All of the resulting *pci* mutants have a growth advantage in FD11 cells and wt growth properties in furin-containing cells. The mutants contain the intact cleavage recognition sequence for furin, and similar to wt virus are unprocessed in FD11 cells and processed in furin-containing CHO cells. When tested in the p62 form, all of the mutants showed membrane fusion activity at a significantly higher pH than that of the wt/p62 virus. Detailed studies of the low pH-induced conformational

changes in one mutant, *pci-4*, demonstrated that, as predicted from its fusion phenotype, the mutation(s) destabilized the *pci-4* p62–E1 dimer and allowed E1 homotrimer formation at a substantially higher pH and efficiency compared to the wt/p62 virus. Taken together, these data suggest that the increased growth of all 7 *pci* mutants in FD11 cells is the result of dimer destabilization leading to E1 trimerization and fusion at a higher pH.

A number of other resuscitating mutations of alphaviruses have been isolated based on initial mutations in p62 or PE2 that block furin cleavage. In addition to their effects on fusion due to the lack of p62 processing, such mutations in the furin cleavage site can also have pleiotropic effects. The unprocessed furin cleavage recognition sequence mediates virion attachment to cell surface heparan sulfate (Klimstra et al., 1999). Mutations within this region thus not only block virus envelope protein processing but also decrease the binding of p62 virus to host cells and may change the conformation of the virus envelope proteins (Klimstra et al., 1999; Salminen et al., 1992; Zhang et al., 2003). Comparison of the results from these systems with the mutations identified in our studies points out interesting parallels and differences.

Studies on revertants of the cleavage-deficient SFV mutant SHQL identified both mutations that restored p62 processing and also four second-site suppressor mutations (Tubulekas and Liljeström, 1998). The suppressor mutations E3 H64R and E2 Q4R do not have effects on dimer stability, and the underlying reason for increased virus infectivity is unknown. The R244I and R244K mutations were found to destabilize the p62–E1 heterodimer at any pH, similar to our findings with *pci-4*. The Sindbis virus cleavage mutant TRSB-N has acquired a new glycosylation site adjacent to the cleavage site and produces p62 virus with a strongly acid-shifted pH threshold (Heidner et al., 1994; Russell et al., 1989; Smit et al., 2001). Revertants of TRSB-N either restore PE2 cleavage or acquire a variety of second-site mutations (C25R on E3; H169L and T198M on E2; P191T on E2; N239H on E2; D82G and E216G on E2) that shift TRSB-N fusion and homotrimer formation back towards the wt pH threshold (Heidner et al., 1994; Smit et al., 2001). However, it appears that the resuscitating mutations isolated in this system (C25R in E3, and P191T, T198M, E216G, N239H in E2) are specific for the TRSB-N mutation, rather than generally compensating for unprocessed PE2 (Heidner et al., 1994). Revertant studies on a Venezuelan equine encephalitis virus cleavage mutant identified two second-site resuscitating mutations: L243Q on E2 and F253S on E1 (Davis et al., 1995). The resuscitating effects of F253S also appear to be specific for the original cleavage-defective mutant used for the selection.

The *pci* mutant selection uses the FD11 cells' furin deficiency rather than a mutation to block p62 cleavage. Thus, by definition all of the *pci* mutants have resuscitating effects in the context of the wt sequence, and there is no selection for revertants that restore a mutated cleavage site. Although in theory the *pci* mutants could have acquired

sequence alterations leading to cleavage by another cellular enzyme, all of the mutations we isolated affected virus fusion properties rather than processing itself. Previous in vitro enzyme digestion studies showed that p62 was significantly more susceptible to cleavage by furin than by hSPC7, another cellular endoprotease of comparable specificity, and was also readily cleaved by trypsin (Zhang et al., 2003). The lack of alternative cleavage mechanisms in the *pci* mutants may demonstrate that a suitable alternative protease was not available in the secretory pathway of the FD11 cells, or simply that mutations that allow fusion at a higher pH arose more easily than those that permit alternative processing.

Structural studies have clearly indicated important interactions between E2 and E1 (Lescar et al., 2001; Zhang et al., 2002). A major interface occurs between the tip region containing the fusion peptide in the E1 domain II and the E2 projecting domain. There is a gap in the dimer interface followed by an interaction of E1 domain III with E2, and then extensive interactions between the stem and transmembrane (TM) domains of the E1 and E2 proteins. All of the E2 *pci* mutations were in the N-terminal half of the E2 protein, and the resuscitating mutations identified in SIN and VEE are also located primarily in the N-terminal half of E2. Two residues, E2 H170 and R244, are interesting as they were identified in both the current selections and in previous resuscitating mutant selections, although the specific substitutions vary. Perhaps surprisingly, our pci mutant study and other resuscitating studies in SIN and VEE have not identified mutations in the stem and TM segments of E2 or E1. However, the interaction of E2 and E1 in these regions has been shown to play a role in alphavirus assembly and budding (Yao et al., 1996), and a recent study demonstrated that TM mutations destabilized the E2–E1 dimer but produced less efficient fusion (Sjoberg and Garoff, 2003). Thus, important roles of the E1 and E2 stem and TM regions in virus assembly and fusion could act against the selection of *pci* mutations in these domains.

It is striking that in a variety of selections for mutations that compensate for the block in p62 cleavage, only three mutations in the E1 protein have been identified: two in domain I at positions 11 and 159 (Fig. 2), and one in domain II at position 253 (Davis et al., 1995). There may be several reasons for this distribution. E1 is critical for the formation of the icosahedral glycoprotein lattice and thus for virus budding (Ekstrom et al., 1994; Lescar et al., 2001; Pletnev et al., 2001; Zhang et al., 2002). As E1 is the fusion protein, it also contains key structural motifs for trimerization and target membrane interaction. Thus, E1 may be less permissive for mutations than E2. Studies of the E1 ectodomain indicate that low pH has independent effects on E1 (Gibbons et al., 2004a; Glomb-Reinmund and Kielian, 1998; Klimjack et al., 1994). The phenotype of p62 virus indicates that dimer dissociation is an early step in fusion that occurs prior to the E1 protein responding to low pH, inserting into the target membrane, and trimerizing

(Salminen et al., 1992; Zhang et al., 2003). It may be that low pH-induced dimer dissociation reflects primarily conformational changes in the E2 protein, thus making it the predominant location of the resuscitating mutations.

Cryo-EM studies demonstrate clear conformational changes that take place upon p62 processing (Ferlenghi et al., 1998), but it is not clear how many of the heterodimeric contacts are altered when p62 is cleaved. The *pci-4* heterodimer was destabilized when assayed in either the p62 or E2 form, suggesting that at least some of the dimer interactions are conserved between the processed and unprocessed conformations. However, in contrast to results with the p62 virus preparations, we observed only marginal effects of any of the *pci* mutations on the fusion of processed virus. There may be an upper limit to the dimer effects and pH-shift of the *pci* mutants, since presumably any E1 proteins that would be susceptible to fusion at the pH of the trans-Golgi network would be inactivated. Determining the effects of *pci* mutations on the E2 dimer interaction would be one approach to defining the alterations in dimer contacts during virus maturation.

## Materials and methods

### Cells

BHK-21 cells were cultured as previously described (Zhang et al., 2003). The FD11 cell line and its parental cell line (CHO-K1) (Gordon et al., 1995) were kindly provided by Dr. Stephen H. Leppla at the National Institutes of Health, and cultured at 37 °C as previously described (Zhang et al., 2003), in α-minimal essential medium, supplemented with 10% fetal bovine serum (FBS) and 100 U penicillin and 100 μg streptomycin per ml (P/S).

### Mutant virus selection, isolation and sequencing

To select p62-cleavage-independent (*pci*) SFV mutants, FD11 cells were plated on ten 35-mm-diameter plates and each plate was infected with wt SFV at 0.01 PFU per cell at 37 °C for 1.5 h in Medium 1 (MEM supplemented with 0.2% BSA, P/S, 40 mg proline per liter, and 10 mM HEPES, pH 7.0). Following infection, cells were washed four times with 2 ml Medium 1, and then incubated for 15 h at 37 °C in 2 ml Medium 1. The medium was collected from each plate and cell debris was removed by centrifugation at 14,000 rpm for 15 min at 4 °C in an Eppendorf Centrifuge 5417C. The titer of progeny virus in the medium from each plate was determined by plaque assay on BHK cells. Virus from each of the 10 plates was then used to infect new FD11 cells at a multiplicity of 0.01 PFU/cell as described above, and the selection in FD11 cells was repeated for a total of 10 cycles. At the end of the selection, all 10 selected virus stocks produced small but distinct plaques when assayed on FD11 cells, while the wt virus did not form plaques. To

isolate mutants from the selected stocks, viruses were plaqued on FD11 cells at 37 °C under an agarose overlay containing 0.7% low-melting-point agarose, MEM, P/S, 5% FBS and 4.4 g NaHCO₃ per liter. Isolated plaques were picked and amplified in FD11 cells in a 24-well tray at 37 °C. The expanded stocks were evaluated by plaque assay on FD11 cells. For those isolates that formed plaques on FD11 cells (*pci-1*, *-2*, *-4*, *-5*, *-6*, *-7*, and *-8*), a second round of plaque purification was performed. No *pci* mutants were isolated from plates 3, 9, and 10.

Viral genomic RNA isolation and sequence analysis were performed essentially as previously described (Ahn et al., 1999; Glomb-Reinmund and Kielian, 1998; Ou et al., 1981). In brief, each *pci* mutant was propagated by infecting one 75-cm² flask of FD11 cells at 0.01 PFU/cell using a p62 stock prepared in FD11 cells. Cell debris was removed by centrifugation and viruses were then pelleted by centrifugation for 1 h at 40,000 rpm in an SW41 rotor at 4 °C. Viral RNA was isolated and viral cDNA was prepared and amplified by reverse transcription (RT)-PCR. Both strands of the cDNA encompassing the C-terminal half of the capsid and the entire p62-6k-E1 region were sequenced in the Einstein automated DNA sequencing facility. All sequence changes were verified by a second independent RT-PCR and sequence analysis.

### Viruses

wt SFV was a well characterized, plaque-purified isolate (Glomb-Reinmund and Kielian, 1998). Unprocessed, p62-containing wt SFV (wt/p62) and *pci* mutants (*pci*/p62) were prepared by virus propagation in FD11 cells as described previously (Zhang et al., 2003). To prepare *pci*/E2 virus stocks, BHK cells were infected with *pci*/p62 viruses at 1 PFU per cell at 37 °C for 1.5 h. The cells were then washed, incubated in MEM plus 10 mM HEPES pH 7.5 and 0.2% BSA for an additional 20 h, and the virus stock harvested as previously described (Zhang et al., 2003). [³⁵S]methionine/cysteine-labeled wt/p62 and *pci-4*/p62 or *pci-4*/E2 viruses were prepared in FD11 or BHK cells, and were harvested and gradient-purified as previously described (Duffus et al., 1995; Zhang et al., 2003).

### Assays of virus processing, fusion, E1 homotrimerization

Processing of the envelope protein p62 was assayed by pulse-chase analysis as previously described (Zhang et al., 2003). In brief, FD11 cells or CHO cells were infected with wt or *pci* mutants at 10 PFU per cell for 8h at 37 °C, pulse-labeled with 50 μCi of [³⁵S]methionine-cysteine per ml for 20 min and then chased in the absence of label for 6 h. The chase media were immunoprecipitated with a polyclonal antibody against the SFV envelope proteins, and the samples were analyzed by SDS-PAGE and fluorography (Kielian et al., 1990).

Virus fusion with the plasma membrane was assayed essentially as previously described (Zhang et al., 2003). In

brief, serial dilutions of virus were bound on ice to BHK cells, treated with media at the indicated pH at 37 °C for 3 min to trigger virus–plasma membrane fusion, and then cultured overnight at 28 °C in the presence of 20 mM NH$_4$Cl to prevent secondary infection. The infected cells were quantitated by immunofluorescence microscopy. Data shown are the average of triplicate samples for each point.

E1 homotrimer formation was assayed using the resistance of the trimer to disruption by SDS sample buffer at 30 °C (Gibbons et al., 2000; Wahlberg and Garoff, 1992). Radiolabeled virus was mixed with 0.8 mM complete liposomes and the mixture was treated at the indicated pH for 5 min at 37 °C. Samples were adjusted to neutral pH on ice, and solubilized for 3 min in SDS sample buffer at 30 °C. Samples were analyzed by SDS-PAGE, and homotrimer formation was quantitated by phosphorimager analysis.

## Assay for p62 and E1 dimer stability

Purified radiolabeled viruses were diluted in buffer containing 10 mM Tris (pH 8.0) and 1 mM MgCl$_2$ on ice. A pretitrated volume of 0.5 N acetic acid was added to adjust the sample to the indicated final pH, and the mixture was incubated for 10 min on ice. Viruses were directly solubilized in 1% Triton X-100 and 150 mM NaCl for 10 min on ice and then readjusted to neutral pH with a precalibrated volume of 0.5 N NaOH (Wahlberg et al., 1989). Samples were immunoprecipitated with the anti-E1 monoclonal antibody (mAb) E1-1 or the anti-E2 mAb E2-3, and analyzed by SDS-PAGE (Duffus et al., 1995).

## Acknowledgments

## References

Ahn, A., Klimjack, M.R., Chatterjee, P.K., Kielian, M., 1999. An epitope of the Semliki Forest virus fusion protein exposed during virus-membrane fusion. J. Virol. 73, 10029–10039.

Andersson, H., Barth, B.U., Ekström, M., Garoff, H., 1997. Oligomerization-dependent folding of the membrane fusion protein of Semliki Forest virus. J. Virol. 71, 9654–9663.

Blumenthal, R., Clague, M.J., Durell, S.R., Epand, R.M., 2003. Membrane fusion. Chem. Rev. 103, 53–69.

Carleton, M., Lee, H., Mulvey, M., Brown, D.T., 1997. Role of glycoprotein PE2 in formation and maturation of the Sindbis virus spike. J. Virol. 71, 1558–1566.

Cheng, R.H., Kuhn, R.J., Olson, N.H., Rossman, M.G., Choi, H.-K., Smith, T.J., Baker, T.S., 1995. Nucleocapsid and glycoprotein organization in an enveloped virus. Cell 80, 621–630.

Davis, N.L., Brown, K.W., Greenwald, G.F., Zajac, A.J., Zacny, V.L., Smith, J.F., Johnston, R.E., 1995. Attenuated mutants of venezuelan equine encephalitis virus containing lethal mutations in the PE2 cleavage signal combined with a second-site suppressor mutation in E1. Virology 212, 102–110.

DeTulleo, L., Kirchhausen, T., 1998. The clathrin endocytic pathway in viral infection. EMBO J. 17, 4585–4593.

Duffus, W.A., Levy-Mintz, P., Klimjack, M.R., Kielian, M., 1995. Mutations in the putative fusion peptide of Semliki Forest virus affect spike protein oligomerization and virus assembly. J. Virol. 69, 2471–2479.

Eckert, D.M., Kim, P.S., 2001. Mechanisms of viral membrane fusion and its inhibition. Annu. Rev. Biochem. 70, 777–810.

Ekstrom, M., Liljeström, P., Garoff, H., 1994. Membrane protein lateral interactions control Semliki Forest virus budding. EMBO J. 13, 1058–1064.

Ferlenghi, I., Gowen, B., Haas, F.D., Mancini, E.J., Garoff, H., Sjoberg, M., Fuller, S.D., 1998. The first step: maturation of the Semliki Forest virus spike occurs through a dramatic localized conformational change. J. Mol. Biol. 283, 71–81.

Fuller, S.D., Berriman, J.A., Butcher, S.J., Gowen, B.E., 1995. Low pH induces swiveling of the glycoprotein heterodimers in the Semliki Forest virus spike complex. Cell 81, 715–725.

Gibbons, D.L., Ahn, A., Chatterjee, P.K., Kielian, M., 2000. Formation and characterization of the trimeric form of the fusion protein of Semliki Forest virus. J. Virol. 74, 7772–7780.

Gibbons, D.L., Erk, I., Reilly, B., Navaza, J., Kielian, M., Rey, F.A., Lepault, J., 2003. Visualization of the target-membrane-inserted fusion protein of Semliki Forest virus by combined electron microscopy and crystallography. Cell 114, 573–583.

Gibbons, D.L., Ahn, A., Liao, M., Hammar, L., Cheng, R.H., Kielian, M., 2004a. Multistep regulation of membrane insertion of the fusion peptide of Semliki Forest virus. J. Virol. 78, 3312–3318.

Gibbons, D.L., Vaney, M.-C., Roussel, A., Vigouroux, A., Reilly, B., Lepault, J., Kielian, M., Rey, F.A., 2004b. Conformational change and protein–protein interactions of the fusion protein of Semliki Forest virus. Nature 427, 320–325.

Glomb-Reinmund, S., Kielian, M., 1998. fus-1, a pH-shift mutant of Semliki Forest virus, acts by altering spike subunit interactions via a mutation in the E2 subunit. J. Virol. 72, 4281–4287.

Gordon, V.M., Klimpel, K.R., Arora, N., Henderson, M.A., Leppla, S.H., 1995. Proteolytic activation of bacterial toxins by eukaryotic cells is performed by furin and by additional cellular proteases. Infect. Immun. 63, 82–87.

Heidner, H.W., McKnight, K.L., Davis, N.L., Johnston, R.E., 1994. Lethality of PE2 incorporation into Sindbis virus can be suppressed by second-site mutations in E3 and E2. J. Virol. 68, 2683–2692.

Helenius, A., Kartenbeck, J., Simons, K., Fries, E., 1980. On the entry of Semliki Forest virus into BHK-21 cells. J. Cell Biol. 84, 404–420.

Hernandez, L.D., Hoffman, L.R., Wolfsberg, T.G., White, J.M., 1996. Virus–cell and cell–cell fusion. Annu. Rev. Cell Dev. Biol. 12, 627–661.

Jain, S.K., DeCandido, S., Kielian, M., 1991. Processing of the p62 envelope precursor protein of Semliki Forest virus. J. Biol. Chem. 266, 5756–5761.

Justman, J., Klimjack, M.R., Kielian, M., 1993. Role of spike protein conformational changes in fusion of Semliki Forest virus. J. Virol. 67, 7597–7607.

Kielian, M., 1995. Membrane fusion and the alphavirus life cycle. Adv. Virus Res. 45, 113–151.

Kielian, M.C., Keränen, S., Kääriäinen, L., Helenius, A., 1984. Membrane fusion mutants of Semliki Forest virus. J. Cell Biol. 98, 139–145.

Kielian, M., Jungerwirth, S., Sayad, K.U., DeCandido, S., 1990. Biosynthesis, maturation, and acid-activation of the Semliki Forest virus fusion protein. J. Virol. 64, 4614–4624.

Kielian, M., Klimjack, M.R., Ghosh, S., Duffus, W.A., 1996. Mechanisms of mutations inhibiting fusion and infection by Semliki Forest virus. J. Cell Biol. 134, 863–872.

Kielian, M., Chatterjee, P.K., Gibbons, D.L., Lu, Y.E., 2000. Specific roles for lipids in virus fusion and exit: examples from the alphaviruses. In: Hilderson, H., Fuller, S. (Eds.), Subcellular Biochemistry, Fusion of Biological Membranes and Related Problems, vol. 34. Plenum Publishers, New York, pp. 409–455.

Klimjack, M.R., Jeffrey, S., Kielian, M., 1994. Membrane and protein interactions of a soluble form of the Semliki Forest virus fusion protein. J. Virol. 68, 6940–6946.

Klimstra, W.B., Heidner, H.W., Johnston, R.E., 1999. The furin protease cleavage recognition sequence of Sindbis virus PE2 can mediate virion attachment to cell surface heparan sulfate. J. Virol. 73, 6299–6306.

Lescar, J., Roussel, A., Wien, M.W., Navaza, J., Fuller, S.D., Wengler, G., Rey, F.A., 2001. The fusion glycoprotein shell of Semliki Forest virus: an icosahedral assembly primed for fusogenic activation at endosomal pH. Cell 105, 137–148.

Lobigs, M., Garoff, H., 1990. Fusion function of the Semliki Forest virus spike is activated by proteolytic cleavage of the envelope glycoprotein precursor p62. J. Virol. 64, 1233–1240.

Lu, Y.E., Eng, C.H., Shome, S.G., Kielian, M., 2001. In vivo generation and characterization of a soluble form of the Semliki forest virus fusion protein. J. Virol. 75, 8329–8339.

Mancini, E.J., Clarke, M., Gowen, B.E., Rutten, T., Fuller, S.D., 2000. Cryo-electron microscopy reveals the functional organization of an enveloped virus, Semliki forest virus. Mol. Cell 5, 255–266.

Marsh, M., Helenius, A., 1980. Adsorptive endocytosis of Semliki Forest virus. J. Mol. Biol. 142, 439–454.

Molinari, M., Helenius, A., 2000. Chaperone selection during glycoprotein translocation into the endoplasmic reticulum. Science 288, 331–333.

Ou, J.-H., Strauss, E.G., Strauss, J.H., 1981. Comparative studies of the 3′-terminal sequences of several alphavirus RNAs. Virology 109, 281–289.

Pletnev, S.V., Zhang, W., Mukhopadhyay, S., Fisher, B.R., Hernandez, R., Brown, D.T., Baker, T.S., Rossmann, M.G., Kuhn, R.J., 2001. Locations of carbohydrate sites on alphavirus glycoproteins show that E1 forms an icosahedral scaffold. Cell 105, 127–136.

Russell, D.L., Dalrymple, J.M., Johnston, R.E., 1989. Sindbis virus mutations which coordinately affect glycoprotein processing, penetration, and virulence in mice. J. Virol. 63, 16l9–1629.

Salminen, A., Wahlberg, J.M., Lobigs, M., Liljeström, P., Garoff, H., 1992. Membrane fusion process of Semliki Forest virus II: cleavage-dependent reorganization of the spike protein complex controls virus entry. J. Cell Biol. 116, 349–357.

Schlesinger, S., Schlesinger, M.J., 2001. Togaviridae: the viruses and their replication. In: Knipe, D.M., Howley, P.M. (Eds.), Fields Virology. Lippincott, Williams and Wilkins, Philadelphia, pp. 895–916.

Sieczkarski, S.B., Whittaker, G.R., 2002. Influenza virus can enter and infect cells in the absence of clathrin-mediated endocytosis. J. Virol. 76, 10455–10464.

Sjoberg, M., Garoff, H., 2003. Interactions between the transmembrane segments of the alphavirus E1 and E2 proteins play a role in virus budding and fusion. J. Virol. 77, 3441–3450.

Smit, J.M., Klimstra, W.B., Ryman, K.D., Bittman, R., Johnston, R.E., Wilschut, J., 2001. PE2 cleavage mutants of Sindbis virus: correlation between viral infectivity and pH-dependent membrane fusion activation of the spike heterodimer. J. Virol. 75, 11196–11204.

Strauss, J.H., Strauss, E.G., 1994. The alphaviruses: gene expression, replication, and evolution. Microbiol. Rev. 58, 491–562.

Tubulekas, I., Liljeström, P., 1998. Suppressors of cleavage-site mutations in the p62 envelope protein of Semliki Forest virus reveal dynamics in spike structure and function. J. Virol. 72, 2825–2831.

Vashishtha, M., Phalen, T., Marquardt, M.T., Ryu, J.S., Ng, A.C., Kielian, M., 1998. A single point mutation controls the cholesterol dependence of Semliki Forest virus entry and exit. J. Cell Biol. 140, 91–99.

Wahlberg, J.M., Garoff, H., 1992. Membrane fusion process of Semliki Forest virus I: low pH-induced rearrangement in spike protein quaternary structure precedes virus penetration into cells. J. Cell Biol. 116, 339–348.

Wahlberg, J.M., Boere, W.A.M., Garoff, H., 1989. The heterodimeric association between the membrane proteins of Semliki Forest virus changes its sensitivity to low pH during virus maturation. J. Virol. 63, 4991–4997.

Wahlberg, J.M., Bron, R., Wilschut, J., Garoff, H., 1992. Membrane fusion of Semliki Forest virus involves homotrimers of the fusion protein. J. Virol. 66, 7309–7318.

Yao, J.S., Strauss, E.G., Strauss, J.H., 1996. Interactions between PE2, E1, and 6K required for assembly of alphaviruses studied with chimeric viruses. J. Virol. 70, 7910–7920.

Zhang, W., Mukhopadhyay, S., Pletnev, S.V., Baker, T.S., Kuhn, R.J., Rossmann, M.G., 2002. Placement of the structural proteins in Sindbis virus. J. Virol. 76, 11645–11658.

Zhang, X., Fugere, M., Day, R., Kielian, M., 2003. Furin processing and proteolytic activation of Semliki Forest virus. J. Virol. 77, 2981–2989.

Zhao, H., Garoff, H., 1992. Role of cell surface spikes in alphavirus budding. J. Virol. 66, 7089–7095.